

EXPERIMENTAL INVESTIGATIONS IN ELECTRIC DISCHARGE MACHINING OF INCONEL-X 750 USING HYBRID OPTIMIZATION APPROACH

Kuldeep Kumar, Jogendra Kumar, Rajesh Kumar Verma

Department of Mechanical Engineering, Madan Mohan Malviya University of Technology, Gorakhpur-273010, India

Corresponding author: Rajesh Kumar Verma, rkvme@mmmut.ac.in

Abstract: Inconel alloys are used in different manufacturing applications such as dissipate structures of petrol engines, thermal reactors, built combustion chambers, etc. Electric discharge machining (EDM) is mainly employed to obtain high precision in complex shapes of very hard material that cannot be machined by traditional machining approaches. In this paper, an effort has been made to study the machining aspect of Inconel X-750 and the simultaneous optimization of machining characteristics. According to Taguchi L_{16} Orthogonal array (OA) experimental design, the machining run order was performed using the copper electrode. Machining performances were considered as Material removal rate (MRR), Tool wear rate (TWR), and Surface roughness (Ra). An integrated approach of the Principal component analysis and Technique for order of preference by similarity to ideal solution based Taguchi theory (PCA-TOPSIS-Taguchi) gives optimum parametric settings as Input current (I)-16 A, Pulse on Time (P) -400 μ s, Duty cycle (D)-10 % & Voltage (V)-70 volts. Analysis of variance (ANOVA) has been used to study the influence of machine parameters on EDM quality characteristics. The confirmatory test shows that the outcomes of the hybrid module show satisfactory agreement in optimized value. This integrated approach can be endorsed for offline and online quality and productivity monitoring.

Key words: PCA, TOPSIS, EDM, Inconel X-750, ANOVA.

1. INTRODUCTION

Inconel alloys are used in various functions such as aircraft engine parts, space technology, and satellite components due to their superior specific strength at a very high range of temperature and pressure (Payal, Maheshwari, & Bharti, 2019; Shandilya & Rouniyar, 2020). During prolonged interaction with temperature and pressure, many alloys start a crack, corrode, deform, creep, etc. but at this stage. Inconel alloys possess entrance resistance to these critical issues (Jozić, Dumanić, & Bajić, 2020). EDM played a significant role in manufacturing operations, like cutting and shape, die, tool, and mold-making (Kumar, Pandey, & Sharma, 2019). EDM processes are also commonly used nowadays in the aerospace, automobile, sports,

biomedical and mold-making industries of difficult to machine materials (Moharana & Patro, 2019).

Electrical energy is used to produce a spark and removal of material is possible mainly due to the spark's thermal energy (Phate, Toney, & Phate, 2020). The workpiece and the electrode (such as deionized water, kerosene, etc.) are submerged in a dielectric fluid (Abdul-Rani, Razak, Littlefair, Gibson, & Nanimina, 2017; Kolli & Kumar, 2015; A. K. Sahu & Mahapatra, 2018). During the machining processes, the tool acts as a cathode, and the workpiece serves as an anode. During machining processes, the material removal takes place from the workpiece by melting and evaporation due to the formation of spark between tool and workpiece. There is no interaction between the tool and the workpiece throughout the machining activity. The electrical discharge process is a thermal phenomenon that extracts material from the workpiece and affects the heat-affected zone's metallurgical properties (HAZ). Various scholars like (Diyaley & Chakraborty, 2019; N. Singh, Routara, & Das, 2018; Srinivasan, Mohammad Chand, Deepan Bharathi Kannan, Sathiya, & Biju, 2018), etc. examined the best process parameter combination, i.e., high MRR, less tool wear, and improved surface features.

Various pioneer investigators perform their work to select the best tool material and process parameter, but very limited work is available to develop a robust hybrid optimization approach for a correlated response (Chakala, Chandrabose, & Rao, 2019). Sharma et al. used a brass electrode and response surface and genetic algorithm for HSLA. High strength and low alloy steel were used as workpiece material for experimentation. Optimum results were obtained by applying RSM and results were further processed by using a Genetic algorithm. Based on ANOVA analysis, it can be implied that the overcut will decrease as peak current increases due to more discharge. But current increase results in erosion that results in less MRR. With an increase of S.V., discharge energy decreases that also causes a decrease in overcutting. ANOVA proves the significance of the model and the adequacy of results with $r^2=0.98$. (Sivaprakasam, Hariharan, & Gowri,

2014) conducted experiments on μ -EDM to examine the consequence of these factors viz. capacitance, voltage and rate of feed on the performances of S.R., MRR & kerf width. Ti alloy (Ti-6Al-4v) was chosen for the workpiece & used CCD design and RSM for optimization. ANOVA method used to determine the importance of different input factors. It was evident from the result of the experiments that values of input parameters i.e. $V_d=100$ V, $C=10$ nF & feed rate = $15 \mu\text{m/s}$ resulted into the optimum values of the responses which were $\text{MRR} = 0.01802 \text{ mm}^3/\text{min}$, $\text{KF} = 101.5 \mu\text{m}$ and $\text{SR} = 0.789 \mu\text{m}$. Kolli et al. (Kolli & Kumar, 2015) analyzed the effect of mixing graphite powder in dielectric for Ti alloy using Taguchi. Process parameters considered as current, surface concentration and powder concentration and its performance were analyzed based on MRR, S.R. and tool wear. The experiments' results show that MRR shows an increase with an increase in current and powder concentration. In contrast, surface roughness is wholly related to surface concentration, current value, and concentration of the powder. Optimum tool wear is low at current and significantly influenced by surfactant and graphite concentration. Abdul et al. (Abdul-Rani et al., 2017) tried to improve EDM efficiency on A231 Mg alloy for biodegradable manufacturing by using practical mixed EDM (PM-EDM). For controlling the surface roughness, Zn particles are mixed in the dielectric and concluded that pulse on and off Time is the most prominent factor in minimizing roughness. Minimum roughness value is obtained for 2g/L accumulation, 38 A peak current, 16 microsecond Pulse Time, and 256 microsecond pulse time. Particle addition increases the electrode gap increases due to high electric density and dielectric strength decreases. More research is needed for minimizing the high corrosion rate due to the mixing of Zn particles. Goyal et al. (Goyal, 2017) MRR and Surface roughness investigated in a cryogenic electrode WEDM experiment in Inconel 625 and studied the validity of a variety of constraints on MRR and Ra quality. The thickness of the work material & diameter of the Zn coated electrode wire is kept constant by using ANOVA for MRR and Surface roughness. Also, it is observed that, due to the high current density, S.R. shows an increase in pulse on Time. The combination of 12 A active, $125\mu\text{s}$ time pulse and $60\mu\text{s}$ off-time pulse gives the maximum rate of product extraction. Future work extension is feasible by addressing wire fatigue, dimensional accuracy, and surface roughness through other heat treatment. Rajashekar et al. (Rajashekar & Rajaprakash, 2017) performed wire EDM to compare various optimization techniques and study pulse on Time, Pulse off Time, and voltage considered as variables. The Taguchi methods and RSM concept was used to enhance the MRR and minimize Ra. All methods produce the same results and it can be concluded that pulse on Time will have more impact on

MRR, but pulse off Time will have less effect. Risto et al. (Risto, Haas, & Munz, 2016) execute EDM drilling optimization to boost output and precision by drilling equivalent diameter holes using different size electrodes and different current and time discharge combinations. More than the bigger electrode due to high discharge energy, wear in a smaller electrode was found. For minimizing cylindrical deviation, high current is used as compared to high discharge time. Gopala et al. (Gopalakannan, Senthilvelan, & Ranganathan, 2012) used RSM optimization on Al7075-BiC MMC. It was found that S_{ic} value affects MRR and increases electrode wear. MRR first increases on increasing pulse on-Time reach to the maximum and then start to decrease on the increasing pulse on Time. The extremely critical factors for EWR and SR. 49.02 V voltage and 7.77 -microsecond pulse on-time are pulse current and pulse on-time, minimizing S.R. quality. Richard et al. (Richard & Giandomenico, 2018) experimented with predicting the electrode profile and compensating the wear in milling by using rotating electrodes. It can be concluded that the profile of the electrode is related by wear to the trajectory of the tool path, EDM gap and metal material. Jatti et al. (Jatti, 2018) Using the Taguchi L_{18} array for multi-characteristic optimization of Ni-Ti alloy & Ni Cu alloy in EDM. As input parameters, gap current, electrical conductivity, gap voltage, pulse on Time and pulse off Time were taken to control the MRR and TWR. MRR is directly proportional to conductivity and the high value of MRR is obtained at low gap voltage and TWR increases with current and more for low conductivity. Kliuev et al. (Kliuev, Maradia, & Wegener, 2018) performed EDM drilling for non-conducting materials using deionized water as the dielectric. For this purpose, first a conductive layer must be deposited, and it is proposed by material deposit from the electrode. Dressing removes the tool electrode material to achieve the original shape and MRR in this experiment is dependent on the combination of melting, vaporization and thermal stresses, which also causes further distortion. This research may be useful in the near future for cooling holes in the turbine's ceramic curved blades. Koyano et al. (Koyano et al., 2018) To evaluate the temperature of the wire electrode in wire EDM, a bi-color pyrometer experiment was conducted. For calculating wire temperature in wire EDM, a two-colour pyrometer and optical fiber was used. They concluded that if the wire temperature is higher than 1000°C , it is computed by a two-color pyrometer, or if the temperature was lower than 1000°C , under experimental conditions, there is no observation of the temperature by a two-color pyrometer. Zeilmann et al. (Zeilmann, Ivaninski, & Webber, 2018) observed surface integrity of AISI13 in EDM under different pulse time using constant parameters and Cu electrode with different depts. cavity and pulse time, using ANOVA on

collected data. They concluded that different pulse on Time used to make depths cavities. When cavities become deeper and the roughness becomes worse and difficult to remove molten material through flushing. Cracks concentration increases when T_{on} rises. Through the subsurface image, they give two different theories of crack propagation with the ANOVA test. Vincent et al. (Vincent & Kumar, 2016) examined the behavior of En41b on EDM using rotary Cu and brass electrodes. The rotating electrodes of tubular shapes were used in this work. Taguchi L_{16} array and signal to noise ratio for grey relational grade (GRG) and performance was analyzed based on current, pulse off and on Time, gap voltage. The rotation of electrodes improves the machining performance. It is found that tool rotation improves fluidity, wear obtained is more uniform & Ra values obtained are much lower as compared to that obtained with non-rotating electrodes. So centrifugal effects positively affect the performance of EDM. Sahu et al. (J. Sahu, Mohanty, & Mahapatra, 2013) conducted experiments on EDM for different input process parameters. I_d , T_{on} , τ & F_p have been considered for Input process parameters while material removal rate, tool wear rate, Ra and circularity (r_1/r_2) were considered outputs. RSM was adopted for establishing the contribution of different input varying constraints on outputs. It was concluded that the Discharge current gives maximum output and reliability-7 Amp, Pulse on-time-200 μ s, Duty factor-90 percent, & Flushing pressure-0.4 kg / cm^2 was achieved. MRR, TWR and Ra values were obtained as 13.96 mm^3/min , 0.0201 mm^3/min , 4.93 μm , and r_1/r_2 -0.8401.

State of the art concluded that most of the surveys considered MRR, S.R., TWR as machining characteristics and copious effort were done by pioneer researchers in EDM and micro EDM using a different electrode and dielectric medium (Dave, 2019). Outcomes of ANOVA show that machining performance is significantly affected by process parameters and their interaction in these studies. Present findings on GRA, ANN, TOPSIS, Utility, DFA, GA, RSM, shows that uniform priority weight and negligible response correlation has been assumed during the aggregation of conflicting machining performances. These assumptions create nebulousness, inaccuracy, and sloppiness in the results. The exploration of PCA techniques can successfully challenge these types of critical issues. In this paper, the application of the PCA-TOPSIS-Taguchi hybrid approach has been explored to achieve an efficient machining environment during EDM of Inconel X-750. This integrated approach is used to control the MRR, TWR and S.R. for productive machining of Inconel-750. An endeavor has been presented to overcome the drawback and shortcomings of existing Taguchi optimization approaches. This study develops a robust hybrid module for machining performance optimization during EDM processes.

2. MATERIALS AND METHODS

State of the art illustrates that most of the findings were performed the data analysis using traditional Taguchi and other optimization approaches. There is an extreme necessity of a hybrid model using an advanced statistical tools module to achieve a favorable machining environment. An attempt has been made by the PCA-TOPSIS method-based Taguchi method. Manual EDM setup (Figure 1) was used to execute the machining of Inconel X-750. The description of the experimental setup is mentioned in Table 1.

Table 1. Specification of EDM machines

Machine Type	Manual	
Model No	C-3822	
Process Parameter Bounds		
Parameter	Min. Value	Max. Value
Input Current (I)	1 ampere	20 amperes
Pulse on Value (T_{on})	1 μ -second	99 μ -seconds
Pulse off Value (T_{off})	1 μ -second	9 μ -seconds
Voltage (V)	5 volts	60 volts

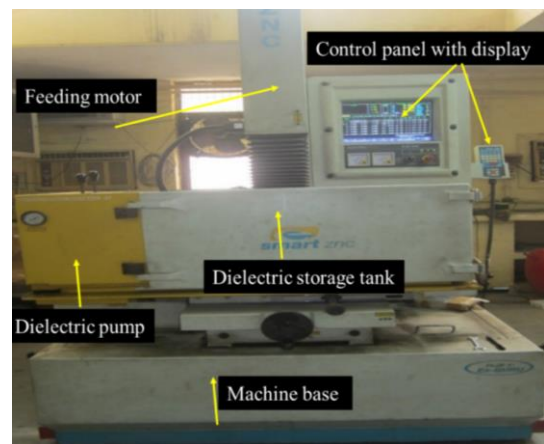


Fig. 1. ZNC EDM Machine (105/06-07)

Inconel X-750 possesses improved properties (Table 2) and chosen as work material, and copper tool with high conductivity, improved machining capability, and low TWR considered in this study. Inconel X-750 lies under nickel-chromium precipitated harden-able alloy. This alloy demonstrates exceptional mechanical properties at an exalted temperature up to 704 degrees Celsius. It is commonly utilized in electrically conducting material, irrespective of size, stiffness, strength and high-performance applications, to shape a very hard substrate and deep hole.

Table 2. Physical properties of Inconel X-750

Factor	value
Density	8.276 g/cm^3
Melting range	1393-1727 $^{\circ}C$
Electrical resistivity	0.3 ohm-cm
Chemical analysis	Ni- 70%, Cr- 14 – 17%, Fe – 5 – 9 %

The surface roughness was measured using the roughness tester (Handy Surf Tokyo Seimitsu) Model No. E-MC-S24B and the material removal rate of Inconel X-750 (density 8.276 g/cm³) were calculated by applying the below expression.

$$MRR = \frac{w_i - w_f}{\rho \times t} \text{ mm}^3/\text{min} \quad (1)$$

Where, w_i, w_f and ρ initial and final weight and density of the sample, respectively. The varying constraints are described in Table 3. According to Taguchi concept experimental design with L₁₆ OA. The pictures of the machined workpiece presented in Figure 2 and the computed experimental data in EDM of Inconel X-750 are depicted in Table 4.

Table 3. Process parameters

Factor	Symbols	Unit	level 1	level 2	level 3	level 4
Input current	I	A	8	12	16	20
Pulse – On - Time	P	μs	200	300	400	500
Duty cycle	D	μs/μs	8	9	10	11
Voltage	V	V	50	60	70	80



Fig. 2. Machined workpiece by copper Tool

Table 4. L₁₆ orthogonal array with observed data

Exp. No.	Input Current (A)	Pulse on Time (μs)	Duty cycle (μs/μs)	Voltage (V)	MRR (mm ³ /min)	TWR (mm ³ /min)	Ra (μm)
1	8	200	8	50	0.1381	0.0019	3.4
2	8	300	9	60	0.1509	0.001	3.6
3	8	400	10	70	0.2112	0.0048	3.5
4	8	500	11	80	0.1844	0.0034	3.7
5	12	200	9	70	0.2586	0.0041	5.5
6	12	300	8	80	0.1996	0.0027	5.8
7	12	400	11	50	0.3017	0.0041	6.8
8	12	500	10	60	0.3206	0.0088	6.7
9	16	200	10	80	0.3912	0.0133	7
10	16	300	11	70	0.3728	0.0051	6.9
11	16	400	8	60	0.2869	0.0092	7.3
12	16	500	9	50	0.2402	0.0027	7.1
13	20	200	11	60	0.183	0.0033	7.7
14	20	300	10	50	0.2225	0.001	9.2
15	20	400	9	80	0.411	0.0038	9.4
16	20	500	8	70	0.4174	0.0029	9.6

3. METHODOLOGY

3.1 TOPSIS Approach

This method was attempted to optimize the EDM of Inconel X-750 precipitated nickel-chrome alloy. The concept of TOPSIS was based on the optimal estimates of the performance loss of important P.C.s and to find an optimal solution. The PCA-TOPSIS comprises the following stages (Mohapatra & Sahoo, 2018; Taylor, Chakravorty, Gauri, & Chakraborty, 2012).

Step 1: The first step involves the decision Matrix (D.M.) construction.

$$DM = \begin{bmatrix} b_{11} & b_{12} & \cdot & b_{1n} \\ b_{21} & b_{22} & \cdot & b_{2n} \\ \cdot & \cdot & \cdot & \cdot \\ b_{m1} & b_{m2} & \cdot & b_{mn} \end{bmatrix} \quad (2)$$

DM is the decision matrix, n and m is the level and number of individual alternative factor.

Step 2: Formulate a normalized data method (NDM). It shows the relative performance of alternatives generated.

$$NDM = Q_{ij} = \frac{a_{ij}}{\sqrt{\sum_{i=1}^m x_{ij}^2}} \quad (3)$$

Step 3: Determine the matrix of the weighted decision matrix (WDM). WDM is constructed by multiplying by random weights each element of each NDM row.

$$V_{ij} = T_i \times Q_{ij} \quad (4)$$

Step 4: Identify the ideal, positive and neutral solution. The Positive (C+) and the Negative ideal (C-) strategies are defined in accordance with the WDM using the following equations.

$$PIS = C^+ = \{V_1^+, V_2^+ \dots V_n^+\} \quad (5)$$

Where:

$$V_j^+ = \left\{ \left(\max_i(V_{ij}) \text{ if } j \in J \right), \left(\min_i(V_{ij}) \text{ if } j \in J' \right) \right\}$$

$$NI = C^- = \{V_1^-, V_2^- \dots V_n^-\} \quad (6)$$

Where:

$$V_j^- = \left\{ \left(\min_i(V_{ij}) \text{ if } j \in J \right), \left(\max_i(V_{ij}) \text{ if } j \in J' \right) \right\}$$

Step 5: Calculate the distance of separation from each efficient alternative's optimal and non-ideal solution

$$M^+ = \sqrt{\sum_{j=1}^n (V_j^+ - V_{ij})^2} \quad i = 1, \dots, m \quad (7)$$

$$M^- = \sqrt{\sum_{j=1}^n (V_j^- - V_{ij})^2} \quad i = 1, \dots, m \quad (8)$$

Step 6: Measure the relative nearness to the perfect arrangement. The general closeness of the conceivable situation to a perfect arrangement is resolved for every option.

$$P_i = M_i^- / (M_i^+ + M_i^-) \leq P_i \leq 1 \quad (9)$$

Step 7: Score the option according to Ci's value, the lower the proximity value, the higher the score, and thus the better the results.

3.2 PCA-TOPSIS Approach

The TOPSIS-PCA technique improves Inconel X-750's machining efficiency features during Electro Discharge Machining (EDM) by the Taguchi theory. Principal component analysis (PCA) was conducted to minimize correlations of response and convert uncorrelated responses into a smaller number of non-correlated output indices known as major principle components (P.C.s). In TOPSIS, each alternative's separation distance was obtained from both the ideal and the anti-ideal solution. A proximity coefficient against each alternative has been established (Taylor et al., 2012).

PCA is used to define associated information trends and to convey data in ways such as highlighting their similarities and differences with the PCA data; the pattern in the data can be compressed without losing much detail, i.e. reduce the number of dimensions (Chatterjee, Mondal, Boral, Banerjee, & Chakraborty, 2017). The basic steps of the PCA are discussed below.

- (i.) Acquisition of certain data
- (ii.) Data Normalization
- (iii.) Covariance matrix calculation
- (iv.) Interpreting the covariance matrix

(a). The correlation coefficient array calculation is calculated using the following equation:

$$R_{ij} = \frac{Cov\{A_i(j), A_i(l)\}}{\sigma_{(ai)}(j) \times \sigma_{(ai)}(l)} \quad j = 1 \text{ to } n \text{ and } l = 1 \text{ to } n \quad (10)$$

In equation (10) $Cov\{A_i(j), A_i(l)\}$ are the covariance of sequences $A_i(j)$ and $A_i(l)$ respectively; and $\sigma_{(ai)}(l)$ denotes the S.D of sequence $A_i(l)$.

(b). Individual values and individual vectors were determined using the set of correlation coefficients:

$$(R - \lambda_k I_m) V_{ik} = 0 \quad (11)$$

In equation (11) λ_k represents eigenvalues; $\sum_{k=1}^n \lambda_k = n$ and $k = 1$ to n ; the term V_{ik} represents $V_{ik} = [a_{k1} a_{k2} \dots a_{kn}]^{k=1 \text{ to } n}$ eigenvectors corresponding to eigenvalues λ_k (Umamaheswarrao, Dantuluri, Koka, & Bhuvanagiri, 2019).

(c). Finally, the main components were calculated using the following equation:

$$Y_{mk} = \sum_i X_{m(i)} \times V_{ik} \quad (12)$$

The equation (12) produces y_{m1} as the first P.C., y_{m2} as the second P.C., and so on.

4. RESULTS AND DISCUSSIONS

This study shows the development of multi-objective optimization modules during EDM of InconelX-750, namely TOPSIS- PCA hybrid module for the combination of various conflicting responses into a single objective function using Minitab-18 software. The machining performance considered in this work is MRR, TWR, and Ra. The details of TOPSIS and PCA modules are mentioned in the below section.

A decision matrix is designed using equation (2) and using equation (3) is used for normalizing data method. After data normalize, using equations (4) to evaluate the weight matrix for each data of response. There is a multi-criteria decision method used to provide the weight to each response later using equation (9) to calculate the performance index. Here, the desired criteria for MRR is assumed as higher the better (H.B.) and provide the weight (0.35) and TWR, Ra is considered as lower the better (L.B.) criteria as (0.30), (0.35), respectively. The Normalize data, weight matrix, performance index and corresponds ranked are tabulated in Table 5. The result of process parameters on the TOPSIS function was investigated using variance analysis (ANOVA) that is performed at a 95% confidence level. ANOVA for TOPSIS concludes that process parameters input current (I) are significant as p values are less than 0.05 and pulses on Time (P), duty cycle (D) and voltage (V) are insignificant as P is more than 0.05. ANOVA is a statistical method that separates the observed variance information into separate parts for additional testing and also investigates the impact of each constraint on the machining concern. (Mishra & Routara, 2017)(Habib, 2009)(V. Singh, Bhandari, & Yadav, 2017). ANOVA reveals that the P values are less than 0.05 in Table 6 for significant process parameters. It is noted that the input current (I) is the most substantial parameter (83.50%).

Table 5. Normalized matrix and Weighted decision matrix, Pi

Normalize data			Weighted values			Pi
MRR	TWR	Ra	MRR	TWR	Ra	
0.1221	0.0862	0.1258	0.0427	0.0258	0.0440	0.0597
0.1333	0.0470	0.1332	0.0466	0.0141	0.0466	0.0230
0.1867	0.2181	0.1295	0.0653	0.0654	0.0453	0.2739
0.1630	0.1530	0.1369	0.0570	0.0459	0.0479	0.1722
0.2286	0.1877	0.2035	0.0800	0.0563	0.0712	0.3043
0.1765	0.1239	0.2146	0.0617	0.0371	0.0751	0.2101
0.2667	0.1864	0.2516	0.0933	0.0559	0.0880	0.3838
0.2834	0.3999	0.2479	0.0992	0.1199	0.0867	0.6182
0.3458	0.6016	0.2590	0.1210	0.1804	0.0906	0.9196
0.3296	0.2298	0.2553	0.1153	0.0689	0.0893	0.4931
0.2536	0.4156	0.2701	0.0887	0.1246	0.0945	0.6309
0.2123	0.1242	0.2627	0.0743	0.0372	0.0919	0.3003
0.1618	0.1515	0.2849	0.0566	0.0454	0.0997	0.3175
0.1967	0.0450	0.3404	0.0688	0.0135	0.1191	0.3844
0.3634	0.1712	0.3478	0.1271	0.0513	0.1217	0.5842
0.3690	0.1293	0.3552	0.1291	0.0387	0.1243	0.5833

Table 6. ANOVA for TOPSIS

Source	DF	Seq SS	Contribution	F-Value	P-Value
Regression	4	2.7747	84.53%	16.39	0.000
I	1	2.7409	83.50%	5.85	0.032
P	1	0.0026	0.08%	0.05	0.822
D	1	0.0035	0.11%	0.59	0.457
V	1	0.0276	0.84%	0.65	0.435
Error	12	0.5079	15.47%		
Total	16	3.2826	100.00%		

S=0.2057, R-sq=84.53%, R-sq(adj)= 79.37%

The PCA process involves the normalization of the observed data for each performance characteristic using equation (2). Using equation (10), these values are used to determine the matrix of the correlation coefficient and to assign it to additional values. The PCA analysis using equation (11) evaluated the eigenvalue and eigenvector of the normalized data. TOPSIS introduces the principal component assessment (PCA) to show the corresponding significance for each performance feature. PCA implementation specifies the weighted values for each characteristic of the output. The eigenvector value of each response value is reported in Table 7 and each quality attribute's weighting contribution (Table 8) is obtained through the square of the first principal element values of the corresponding eigenvalue.

Table 7. Eigenvalues and their variation

Variable	Eigenvalue	Proportion
MRR	0.639	63.9%
TWR	0.296	29.6%
Ra	0.065	6.5%

Table 8. Eigenvectors for principal components & contribution

Performance characteristic	Eigenvector			Contribution/weighted value
	PC1	PC2	PC3	
MRR	0.683	-0.039	0.729	0.4664
TWR	0.456	0.803	-0.384	0.2079
Ra	0.57	-0.595	-0.567	0.3249

Table 7 indicates the contribution of individual performance for MRR, TWR, and Ra. The first major component's variance contribution among the three performance characteristics is found as the highest (63.9%). The TOPSIS-PCA calculation was obtained using the weighted value of each output characteristic. The aggregated single objective function (Pi) and its corresponding rank are demonstrated in Table 9.

Table 9. Normalized matrix and Weighted decision matrix, Pi

Normalize data			Weighted values			Pi
MRR	TWR	Ra	MRR	TWR	Ra	
0.1221	0.0862	0.1258	0.0570	0.0179	0.0409	0.0469
0.1333	0.0470	0.1332	0.0622	0.0098	0.0433	0.0318
0.1867	0.2181	0.1295	0.0871	0.0454	0.0421	0.2571
0.1630	0.1530	0.1369	0.0761	0.0318	0.0445	0.1626
0.2286	0.1877	0.2035	0.1067	0.039	0.0661	0.3457
0.1765	0.1239	0.2146	0.0823	0.0258	0.0697	0.2288
0.2667	0.1864	0.2516	0.1244	0.0388	0.0818	0.4609
0.2834	0.3999	0.2479	0.1322	0.0832	0.0806	0.6166
0.3458	0.6016	0.2590	0.1613	0.1251	0.0842	0.8854
0.3296	0.2298	0.2553	0.1538	0.0478	0.083	0.6149
0.2536	0.4156	0.2701	0.1183	0.0864	0.0878	0.5972
0.2123	0.1242	0.2627	0.0991	0.0258	0.0854	0.3473
0.1618	0.1515	0.2849	0.0755	0.0315	0.0926	0.3241
0.1967	0.0450	0.3404	0.0918	0.0094	0.1106	0.4267
0.3634	0.1712	0.3478	0.1695	0.0356	0.113	0.7458
0.3690	0.1293	0.3552	0.1722	0.0269	0.1154	0.7573

The effect of the EDM parameters on the performance values is done through variance analysis at a 95% confidence level (Babu, Mathivanan, & Kumar, 2019; Pagar & Gawande, 2020) shown in Table 10. It is noticed that current has the highest impact on the machining characteristics of Inconel X-750. The model F-value of 21.33 corresponding p-value (zero) indicates that the model is significant. ANOVA for PCA-TOPSIS concludes that current (I) are observed noteworthy as p values are less than 0.05, and pulses on Time (P), duty cycle (D) and voltage (V) are insignificant as P values are greater than 0.05. It is remarked that the input (I) current is the most important parameter (86.19%) (Surekha, Sree Lakshmi, Jena, & Samal, 2019).

Table 10. ANOVA for PCA-TOPSIS

Source	DF	Seq SS	Contribution	F-Value	P-Value
Regression	4	3.4333	87.67%	21.33	0.000
I	1	3.3753	86.19%	9.67	0.009
P	1	0.0019	0.05%	0.27	0.610
D	1	0.0260	0.67%	1.39	0.261
V	1	0.0300	0.77%	0.75	0.404
Error	12	0.4829	12.33%		
Total	16	3.9163	100.00%		

S=0.2006, R-sq=87.67%, R-sq(adj)= 83.56%

4.1 Comparative analysis of TOPSIS and PCA-TOPSIS

Based on the confirmatory test outcomes, it is found that under Taguchi L_{16} , TOPSIS-PCA yields different optimal parametric settings. From Table 11, the optimal setting of TOPSIS -Taguchi and TOPSIS-PCA are observed as I-16, P-400, D-10, V-70. The objective function value obtained from TOPSIS- Taguchi and TOPSIS- PCA- are noticed as 0.843382 and 0.882496, respectively. A higher value of the objective function is desired for the TOPSIS-PCA theory's robustness and capability. Table 11 shows that model adequacy for the TOPSIS-PCA (87.67%) is more than the TOPSIS theory (84.53%). Moreover, in the case of error%, the TOPSIS- PCA hybrid approach has obtained a less error value. The proposed integrated optimization tool can be endorsed to achieve a favorable machining environment during EDM of Inconel X-750.

Table 11. Comparative value of TOPSIS and PCA-TOPSIS

Sr. No.	Characteristics	TOPSIS Taguchi	PCA-TOPSIS
1	R ²	84.53%	87.67%,
2	Error	15.47%	12.33%
3	Optimum condition	I-3, P-3, D-3, V-3	I-3, P-3, D-3, V-3
4	Optimum value	0.8433	0.8824

4.2 Response table for PCA-TOPSIS

Table 12 displays the response table for EDM parameters and their optimum levels. The analysis of means from Table 12 indicates that the highest delta value was present (0.4866) (Zurrayen, Mutalib, Idris, Ismail, & Abdul, 2020). The Current parameter (I) on the overall objective function was shown to be the predominant factor accompanied by a pulse on Time (0.1898), voltage (0.1852) and a duty cycle (0.1788). The mean table analysis shows that the optimal machining condition set outside the experiment L_{16} of Taguchi. From Figure 3, the optimal set of input parameters is observed in the current (I) level 3, pulse on time (P) level 3, voltage (V) level 3, and duty cycles (D) level 3.

Table 12. Response Table for average closeness

Level	I	P	D	V
1	0.1246	0.4005	0.4075	0.3204
2	0.4130	0.3255	0.3676	0.3924
3	0.6112	0.5153	0.5464	0.4937
4	0.5635	0.4709	0.3906	0.5056
Delta	0.4866	0.1898	0.1788	0.1852
Rank	1	2	4	3

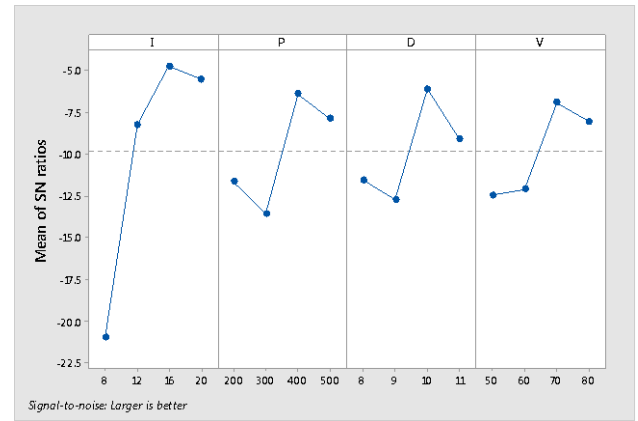


Fig. 3. S/N ratio for TOPSIS- PCA

4.3 Confirmatory tests

The confirmation experiment was staged to check the optimal setting outcomes for PCA-TOPSIS predictions, as shown in Table 13. The objective function solution value obtained from PCA-TOPSIS is found as 0.8824 and a confirmatory test has validated it. It has been remarked that as compared to the initial setting of the I-8, P-200, D-8, V-50 array with objective function as 0.0469. It is found that the MRR increased from 0.1381 to 0.4378 mm³/min, TWR, Ra decreased from 0.0019 to 0.0010 mm³/min and from 3.4 to 3.1 μm, respectively. It was examined as the objective function value is enhanced from 0.0469 to 1.1947 and can be recommended for offline/online quality monitoring during machining of Inconel X-750 in EDM condition.

Table 13. Confirmatory test

Response	PCA-TOPSIS		
	Initial setting	Predicted	Experimental
	I8P200D8V50	I16P400D10V70	I16P400D10V70
MRR	0.1381		0.4378
TWR	0.0019		0.0010
Ra	3.4		3.1
Objective function value	0.0469	0.8824	1.1947

5. CONCLUSIONS

The present study highlights the exploration of an integrated approach by the TOPSIS-PCA-Taguchi theory. Effect of Processes parameter viz. I, P, D, & V and their effects on machining performance, i.e., MRR, TWR and Ra, have been studied competently. The proposed optimizations approach has productively combined the multiple conflicting performances into a single objective function, which is not feasible by the traditional optimization tool and Taguchi concept. PCA has fruitfully used for response priority weight decision and correlation check. The optimal setting obtained through TOPSIS-PCA-Taguchi concept integrated approach are found as Input current -16 A, Pulse on Time - 400 (μs), Duty cycle -10 (μs/μs), Voltage -70 V. The higher value of

the objective function (1.19473) in the proposed optimization tool TOPSIS-PCA-Taguchi shows the high application potential and robustness of the integrated approach in a machining environment. ANOVA has been used to identify the most influencing processes parameter for machining performance. As the developed model is generalized and it can be customized according to machining operation. The TOPSIS-PCA-Taguchi hybridization approach can be praised for quality improvement and productivity concerns in the manufacturing sectors. The proposed integrated approach of the TOPSIS PCA-Taguchi concept model shows high application potential in a machining environment. The involvement of other factors such as different tool material, tool shapes and issues of health and safety may be considered for a more precise interpretation of machining aspects of Inconel X-750. It is designed as a generalized approach; hence, it can be explored for other traditional or non-conventional processes of machining such as drilling, turning, N.C. and CNC machining. This robust method can also be discussed in different case studies of industrial engineering problems in multi attributes decision-making (MADM) context.

6. ACKNOWLEDGMENT

The author is very thankful to the Department of Mechanical Engineering, Madan Mohan Malaviya University of Technology Gorakhpur India, for extending all possible help in carrying out this research work directly or indirectly.

7. ABBREVIATIONS

EDM- Electric Discharge Machining
 OA- Orthogonal Array
 MRR- Material Removal rate
 TWR- Tool wear rate
 Ra- Surface roughness
 PCA- Principle component analysis
 TOPSIS- Technique for Order Preference by Similarity to the Ideal Solution
 I – Input current
 P – Pulse on Time
 D – Duty cycle
 V – Voltage
 ANOVA – Analysis of variance

8. REFERENCES

1. Abdul-Rani, A. M., Razak, M. A., Littlefair, G., Gibson, I., & Nanimina, A. M. (2017). *Improving EDM Process on AZ31 Magnesium Alloy towards Sustainable Biodegradable Implant Manufacturing*. *Procedia Manufacturing*, **7**, pp. 504–509.

<https://doi.org/10.1016/j.promfg.2016.12.05>.

2. Babu, N. S. M., Mathivanan, N. R., Kumar, K. V. (2019). *Influence of machining parameters on the response variable during drilling of the hybrid laminate*, *Australian Journal of Mechanical Engineering*, pp. 1–10. <https://doi.org/10.1080/14484846.2019.1704492>.
3. Chakala, N., Chandrabose, P. S., Rao, C. S. P. (2019). *Optimisation of WEDM parameters on Nitinol alloy using RSM and desirability approach*. *Australian Journal of Mechanical Engineering*, pp. 1–13. <https://doi.org/10.1080/14484846.2019.1681239>.
4. Chatterjee, P., Mondal, S., Boral, S., Banerjee, A., & Chakraborty, S. (2017). *A novel hybrid method for non-traditional machining process selection using factor relationship and multi-attribute border approximation method*, *Facta Universitatis, Series: Mechanical Engineering*, **15**(3), pp. 439–456, <https://doi.org/10.22190/FUME170508024C>.
5. Dave, H. K. (2019). *Optimization of orbital electro discharge machining parameters using TLBO and PSO algorithms*, *International Journal of Modern Manufacturing Technologies*, **11**(2), pp. 19–24.
6. Diyaley, S., Chakraborty, S. (2019). *Optimization of multi-pass face milling parameters using metaheuristic algorithms*. *Facta Universitatis, Series: Mechanical Engineering*, **17**(3), pp. 365–383. <https://doi.org/10.22190/FUME190605043D>.
7. Gopalakannan, S., Senthilvelan, T., Ranganathan, S. (2012). *Modeling and optimization of EDM process parameters on machining of Al7075-B4C MMC using RSM*. *Procedia Engineering*, **38**, pp. 685–690. <https://doi.org/10.1016/j.proeng.2012.06.086>.
8. Goyal, A. (2017). *Investigation of material removal rate and surface roughness during wire electrical discharge machining (WEDM) of Inconel 625 super alloy by cryogenic treated tool electrode*. *Journal of King Saud University - Science*, **29**(4), pp. 528–535. <https://doi.org/10.1016/j.jksus.2017.06.005>.
9. Habib, S. S. (2009). *Study of the parameters in electrical discharge machining through response surface methodology approach*. *Applied Mathematical Modelling*, **33**(12), pp. 4397–4407. <https://doi.org/10.1016/j.apm.2009.03.021>.
10. Jatti, V. S. (2018). *Multi-characteristics optimization in EDM of NiTi alloy, NiCu alloy and BeCu alloy using Taguchi's approach and utility concept*. *Alexandria Engineering Journal*, **57**(4), pp. 2807–2817. <https://doi.org/10.1016/j.aej.2017.11.004>
11. Jozić, S., Dumanić, I., Bajić, D. (2020). *Experimental analysis and optimization of the controllable parameters in turning of en aw-2011 alloy; dry machining and alternative cooling techniques*. *Facta Universitatis, Series: Mechanical Engineering*, **18**(1), pp. 13–29. <https://doi.org/10.22190/FUME191024009J>.
12. Kliuev, M., Maradia, U., Wegener, K. (2018).

- EDM Drilling of Non-Conducting Materials in Deionised Water. *Procedia CIRP*, **68**(April), pp. 11–16. <https://doi.org/10.1016/j.procir.2017.12.014>
13. Kolli, M., Kumar, A. (2015). *Effect of dielectric fluid with surfactant and graphite powder on Electrical Discharge Machining of titanium alloy using Taguchi method*. *Engineering Science and Technology, an International Journal*, **18**(4), pp. 524–535. <https://doi.org/10.1016/j.jestch.2015.03.009>.
14. Koyano, T., Takahashi, T., Tsurutani, S., Hosokawa, A., Furumoto, T., Hashimoto, Y. (2018). *Temperature Measurement of Wire Electrode in Wire EDM by Two-color Pyrometer*. *Procedia CIRP*, **68**(April), pp. 96–99. <https://doi.org/10.1016/j.procir.2017.12.029>
15. Kumar, R., Pandey, A., Sharma, P. (2019). *Investigation of Surface Roughness for Inconel 718 in Blind Hole Drilling with Rotary Tool Electrode*. *Journal of Advanced Manufacturing Systems*, **18**(3), pp. 379–394. <https://doi.org/10.1142/S0219686719500203>.
16. Mishra, B. P., Routara, B. C. (2017). *An experimental investigation and optimisation of performance characteristics in EDM of EN-24 alloy steel using Taguchi Method and Grey Relational Analysis*. *Materials Today: Proceedings*, **4**(8), pp. 7438–7447. <https://doi.org/10.1016/j.matpr.2017.07.075>.
17. Mohapatra, K. D., Sahoo, S. K. (2018). *A multi objective optimization of gear cutting in WEDM of Inconel 718 using TOPSIS method*. *Decision Science Letters*, **7**(2), pp. 157–170. <https://doi.org/10.5267/j.dsl.2017.6.002>.
18. Moharana, B. R., Patro, S. S. (2019). *Multi objective optimization of machining parameters of EN-8 carbon steel in EDM process using GRA method*. *International Journal of Modern Manufacturing Technologies*, **11**(2), pp. 50–56.
19. Pagar, N. D., Gawande, S. H. (2020). *Multi-response design optimisation of convolution stresses of metal bellows using integrated PCA-GRA approach*. *Australian Journal of Mechanical Engineering*, pp. 1–21. <https://doi.org/10.1080/14484846.2020.1725347>.
20. Payal, H., Maheshwari, S., Bharti, P. S. (2019). *Parametric optimization of EDM process for Inconel 825 using GRA and PCA approach*. *Journal of Information and Optimization Sciences*, **40**(2), pp. 291–307. <https://doi.org/10.1080/02522667.2019.1578090>.
21. Phate, M., Toney, S., Phate, V. (2020). *Modelling and investigating the impact of EDM parameters on surface roughness in EDM of Al/Cu/Ni Alloy*. *Australian Journal of Mechanical Engineering*, pp. 1–14. <https://doi.org/10.1080/14484846.2020.1790478>.
22. Rajashekar, R., Rajaprakash, B. M. (2017). *Comparison of optimization techniques of input parameters in wire electrical discharge machining*. *International Journal of Latest Trends in Engineering and Technology*, **8**(41), pp. 149–155. <https://doi.org/10.21172/1.841.26>.
23. Richard, J., Giandomenico, N. (2018). *Electrode Profile Prediction and Wear Compensation in EDM-milling and Micro-EDM-Milling*. *Procedia CIRP*, **68**(April), pp. 819–824. <https://doi.org/10.1016/j.procir.2017.12.162>.
24. Risto, M., Haas, R., Munz, M. (2016). *Optimization of the EDM Drilling Process to Increase the Productivity and Geometrical Accuracy*. *Procedia CIRP*, **42**(Isem Xviii), pp. 537–542. <https://doi.org/10.1016/j.procir.2016.02.247>.
25. Sahu, A. K., Mahapatra, S. S. (2018). *Optimization of electrical discharge machining of titanium alloy (Ti6Al4V) by grey relational analysis based firefly algorithm*. *Additive Manufacturing of Emerging Materials*, pp. 29–53. https://doi.org/10.1007/978-3-319-91713-9_2.
26. Sahu, J., Mohanty, C. P., Mahapatra, S. S. (2013). *A DEA approach for optimization of multiple responses in electrical discharge machining of AISI D2 steel*. *Procedia Engineering*, **51**(NUiCONE 2012), pp. 585–591. <https://doi.org/10.1016/j.proeng.2013.01.083>.
27. Shandilya, P., Rouniyar, A. K. (2020). *Multi-objective parametric optimization on machining of Inconel-825 using wire electrical discharge machining*, pp. 1–13. <https://doi.org/10.1177/0954406220917706>.
28. Singh, N., Routara, B. C., Das, D. (2018). *Study of machining characteristics of Inconel 601 in EDM using RSM*. *Materials Today: Proceedings*, **5**(2), pp. 3438–3449. <https://doi.org/10.1016/j.matpr.2017.11.590>.
29. Singh, V., Bhandari, R., Yadav, V. K. (2017). *An experimental investigation on machining parameters of AISI D2 steel using WEDM*. *International Journal of Advanced Manufacturing Technology*, **93**(1–4), pp. 203–214. <https://doi.org/10.1007/s00170-016-8681-6>.
30. Sivaprakasam, P., Hariharan, P., Gowri, S. (2014). *Modeling and analysis of micro-WEDM process of titanium alloy (Ti-6Al-4V) using response surface approach*. *Engineering Science and Technology, an International Journal*, **17**(4), pp. 227–235. <https://doi.org/10.1016/j.jestch.2014.06.004>.
31. Srinivasan, L., Mohammad Chand, K., Deepan Bharathi Kannan, T., Sathiya, P., Biju, S. (2018). *Application of GRA and TOPSIS Optimization Techniques in GTA Welding of 15CDV6 Aerospace Material*. *Transactions of the Indian Institute of Metals*, **71**(2), pp. 373–382. <https://doi.org/10.1007/s12666-017-1166-y>.
32. Surekha, B., Sree Lakshmi, T., Jena, H., Samal, P. (2019). *Response surface modelling and application*

of fuzzy grey relational analysis to optimise the multi response characteristics of EN-19 machined using powder mixed EDM. Australian Journal of Mechanical Engineering, pp. 1–11. <https://doi.org/10.1080/14484846.2018.1564527>.

33. Taylor, P., Chakravorty, R., Gauri, S. K., Chakraborty, S. (2012). *Materials and Manufacturing Processes Optimization of Correlated Responses of EDM Process Optimization of Correlated Responses of EDM Process.* Materials and Manufacturing Processes, **27**(August 2014), pp. 37–41. <https://doi.org/10.1080/10426914.2011.577875>.

34. Umamaheswarrao, P., Dantuluri, R. R., Koka, N. S. S., Bhuvanagiri, R. S. (2019). *Achieving optimal parametric combination for aisi 52100 steel hard turning with multiple performance characteristics using integrated RSM and GRA-PCA.* International Journal of Modern Manufacturing Technologies, **11**(2), pp. 86–95.

35. Vincent, N., Kumar, A. B. (2016). *Experimental Investigations Into EDM Behaviours of En41b Using Copper and Brass Rotary Tubular Electrode.* Procedia Technology, **25**(Raerest), pp. 877–884. <https://doi.org/10.1016/j.protcy.2016.08.196>.

36. Zeilmann, R. P., Ivaninski, T., Webber, C. (2018). *Surface integrity of AISI H13 under different pulse time and depths by EDM process.* Procedia CIRP, **71**, pp. 472–477. <https://doi.org/10.1016/j.procir.2018.05.031>.

37. Zurrayen, M., Mutalib, A., Idris, M., Ismail, S., Abdul, N. A. (2020). *Multi-objective optimization in friction drilling of aisi1045 steel using grey relational analysis.* International Journal of Modern Manufacturing Technologies, **XII**(1), pp. 75–81.